

# Impact of HRR Radar Processing on Moving Target Identification Performance

**Bart Kahler**  
General Dynamics  
WPAFB, OH 45433

**Erik Blasch**  
Air Force Research Lab  
WPAFB, OH 45433

**Abstract** – Airborne radar tracking in moving ground vehicle scenarios is impacted by sensor, target, and environmental dynamics. Moving targets can be assessed with 1-D High Range Resolution (HRR) Radar profiles with sufficient signal-to-noise (SNR) present which contain enough feature information to discern one target from another to help maintain track or to identify the vehicle. Typical radar clutter suppression algorithms developed for processing moving ground target data not only remove the surrounding clutter but also a portion of the target signature. Enhanced clutter suppression can be achieved using a multi-channel signal subspace (MSS) algorithm which preserves target features. In this paper, we (1) exploit extra information from enhanced clutter suppression for automatic target recognition (ATR), (2) present a gain comparison using displaced phase center antenna (DPCA) and MSS clutter suppressed HRR data; and (3) develop a confusion-matrix identity result for simultaneous tracking and identification (STID). The results show that more channels for MSS increase ID over DCPA, result in a slightly noisier clutter suppressed image, and preserve more target features after clutter cancellation

**Keywords:** radar, clutter suppression, clutter cancellation, space-time adaptive processing (STAP), Displaced Phase Center Antenna (DPCA), multi-channel signal subspace (MSS), automatic target recognition (ATR), High Range Resolution (HRR), moving target identification.

## 1 Introduction

Many surveillance systems incorporate High Range Resolution (HRR) radar and synthetic aperture radar (SAR) modes to be able to capture moving and stationary targets. Feature-, signature-, and categorical-aided tracking and automatic target recognition (ATR) applications benefit from HRR radar processing. Successful simultaneous tracking and identification (STID) [1, 2] applications exploit feature information to determine the target type and dynamics.

To maximize a search area, airborne systems operate at standoff ranges to detect targets and initiate tracks. [3, 4] Tracking systems then transition into a track maintenance mode after target acquisition; however, closely spaced targets such as at road intersections require feature analysis to identify the targets. HRR radar affords dynamic

processing analysis for vehicle tracking and signal features (range, angle, aspect, and peak amplitudes) for target detection and identification.

Pattern recognition algorithms applied to ATR problems are typically trained on a group of desired objects in a library to gain a statistical representation of each objects' features. One dimensional (1-D) HRR classifiers exploit the location and peak amplitude information contained in the HRR signatures [5, 6]. The algorithm then aligns input signatures to the library templates or models [7] and determines the best correlation value for the aligned features. Algorithms often apply a threshold to the best score to reject questionable objects before making identification or class label decisions.

A number of papers have been published that evaluate 1-D HRR ATR solutions [8, 9, 10, 11, 12]. Classifiers have been developed for correlation [13], Bayes and Dempster Shafer information fusion approaches [14], entropy and information theory analysis [15], and Neuro-Fuzzy methods [16]. The classifier results have been used for tracking [17] and multi-look HRR identification [18]. Other approaches include eigen-value template matching [19], Eigen-extended maximum average correlation (EEMACH) filters [20] and likelihood methods accounting for Rician, amplitude, specular, and diffuse, Cisoid scattering [21].

Although the ATR process seems straight forward, misidentification or rejection of an input object as a viable target occurs because of conditions such as the target being obscured from the sensor, targets adjacent to another object, and target transitions from moving to stationary and back to a moving state in a traffic scenario, that unexpectedly alters the features used in the identification process. The importance and impact of extended operating conditions (EOCs) is critical to ATR performance [22]. The quality of the information used in joint tracking, classification, and identification (ID) [23, 24, 25] can be determined through Bayes, Dempster-Shafer, or DSmt analysis methods [26].

HRR ATR algorithm performance is impacted by the quality of the features available in the 1-D HRR profiles. Missing target features in training data will alter the library templates formed resulting in poorer identification performance. The presence of EOCs will degrade 1-D test signatures and the corresponding classifier performance. Since the signature data used by ATR algorithms is not always pristine, information fusion methods have been

developed such as multi-look ATR to enhance ID performance from HRR radar data. Improved HRR processing prior to 1-D HRR profile formation should improve the target features available or reveal more target features, resulting in higher quality 1-D signatures, and improved ATR performance.

This paper reviews HRR data processing in Section 2; discussing the implementation of a standard two-channel DPCA clutter cancellation method, presenting an improved multi-channel signal subspace (MSS) clutter suppression algorithm, and comparing the resulting clutter canceled target chips. In Section 3 a single-look decision level identification method is presented along with performance metrics. Section 4 discusses conclusions and future work.

## 2 HRR Data Processing

Focused 1-D HRR profiles of moving targets may be generated with enhanced target-to-clutter ratios. One such procedure first chips the moving target from the motion compensated video phase history data and aligns the target chips for clutter suppression and focusing. This results in a two dimensional range-Doppler chip that is masked using binary morphology to determine the mean clutter level, target length, and target edges in the chip. The range-Doppler chip is then cropped about the Doppler extent of the target mask before computing the mean of all sub-aperture images. The maximum scatters from each range bin are kept to form the 1-D HRR profile.

Stationary targets from SAR imagery may also be formed into 1-D HRR profiles using a similar process. For targets in SAR imagery, constant-false alarm rate (CFAR) detection is performed first, followed by target mask formation using binary morphology. The formation process crops around the target mask and computes the mean of all sub-aperture images, keeping the maximum scatters from each range bin to form the stationary HRR profile. Shown in **Figure 1** is the general profile formation process flow.

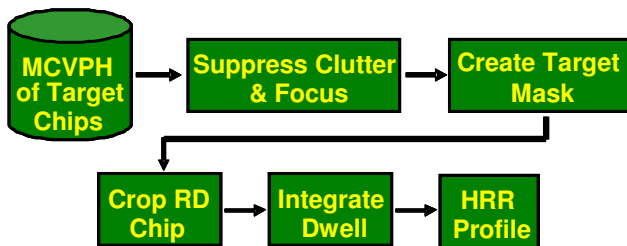


**Figure 1.** 1-D HRR Profile formation Process.

Recent research [6] has shown that HRR profiles formed from SAR imagery of stationary targets have comparable features to profiles of the same moving target at corresponding collection geometries as shown in **Figure 2**.

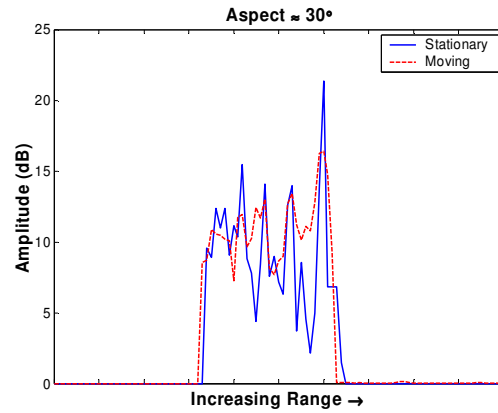


**Figure 2.** Comparison of moving/stationary 1-D HRR profiles.

### 2.1 General Clutter Suppression

Clutter suppression of airborne radar data for moving ground targets is a key step in the target detection and identification processing chain. The goal is to enhance the target signature while reducing the energy of the competing ground clutter surrounding the moving target. Typically, clutter suppression techniques have the unintentional side effect of reducing some of the target energy while suppressing the ground clutter. Although the target-to-clutter ratio may improve greatly, a reduction in the target features is inevitable which impacts target tracking and identification performance further down the processing chain. The processing of airborne multi-channel radar data to cancel the clutter near moving ground targets can be accomplished through a variety of techniques such as Doppler filtering, by space-time adaptive processing (STAP), or displaced phase center antenna (DPCA) processing. [27]

*Doppler filtering* is a technique used with adaptive radars which sense the Doppler distribution of clutter and adjust the radar parameters in an attempt to maximize the signal-to-clutter ratio. Clutter suppression is accomplished by obtaining a separate coherent output from each channel of an antenna array and applying a unique complex weight to each channel. Then the weighted channels are added coherently to cancel the clutter energy. [27, 28, 29]

A two dimensional filtering technique known as *STAP* processing [29, 30, 31, 32] uses the Doppler frequency, sensor platform velocity, and direction of arrival information to achieve clutter cancellation. Adaptive filter weights are determined for the temporal and spatial domains after sampling a coherent train of pulses. These weights then form a two dimensional space-time clutter filter that can be applied to the data to eliminate ground clutter. STAP processing is robust to errors and can simultaneously suppress clutter returns and jamming signals.[33, 34, 35]

In *DPCA* processing the radar motion is compensated for to reduce the Doppler spread of ground clutter induced by the sensor platform. [36, 37, 38] A multi-channel airborne radar configuration often has a pair of antennas positioned so that as the platform travels in time, the

position of the trailing antenna will occupy approximately the same position of the lead antenna at some delta in time. Essentially, for a given time interval, one antenna position is fixed. Clutter suppression is accomplished by subtracting the received signal from the trailing antenna at the delta time from the received signal of the lead antenna at the initial time of the processing interval. [39, 40, 41]

Both STAP and DPCA are capable of cancelling main beam and side lobe clutter for multi-channel airborne radars with two or more antenna phase centers. [33] In this paper, a DPCA two-channel algorithm implementation was chosen for comparison to the multi-channel signal subspace algorithm.

A three channel antenna configuration is shown in Figure 3 where antenna number 1 is the lead channel for the collected data used in this paper. The concept of DPCA processing is illustrated in Figure 3 for a three channel antenna array configuration. The position of the antennas are shown at the initial time,  $t_i$ , and with platform motion the antenna positions at some time interval,  $t_i + \Delta t$  where  $\Delta t$  is the change in time, are shown. Through DPCA processing two antenna positions will appear to be at the same physical location for the array depicted in Figure 3. Therefore, clutter cancellation is possible where channel 2 at  $t_i$  and channel 3 at  $t_i + \Delta t$  line up and where channel 1 at  $t_i$  and channel 2 at  $t_i + \Delta t$  are aligned.

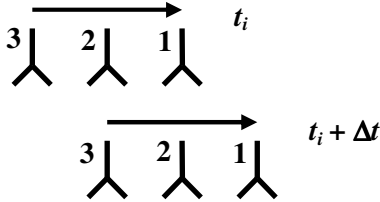


Figure 3. Three-Channel Antenna Configuration.

The radar data processed for this paper was collected at X-Band with the aircraft traveling in a linear flight path north of the scene center collecting in spotlight mode at a depression angle of 8.97 degrees and at a weighted

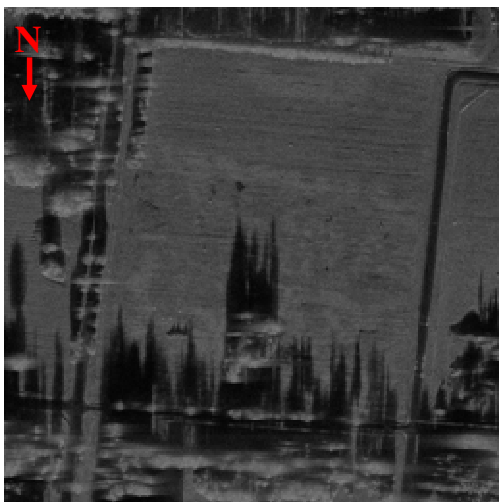


Figure 4. SAR Image of Collection Site.

resolution of approximately 12 inches. As illustrated in the SAR image of Figure 4, the center of the collection site was a rectangular grassy area with roads along the western, eastern, and southern borders of the target area. Wooded areas surround the grassy rectangle along the northern, eastern, and southern portions of the scene. In the scenario, civilian vehicles are traveling along the roads in all directions. The image chips used in the processing discussion are of the test vehicle moving south along the western road.

The two channel DPCA processing approach is explained in Subsection 2.2. Subsection 2.3 explains the multichannel signal subspace algorithm and the clutter suppression results of the target chip presented in Subsection 2.4.

## 2.2 DPCA Technique

In Subsection 2.1 the idea behind DPCA processing was introduced. The DPCA algorithm used in this work was developed for measured data from a radar array of two antennas oriented along the sensor platform path of travel. In general, the data from the trailing antenna is aligned to the lead channel, where the phases are adjusted so that the aligned channels appear to be at the same location in space, and finally the channels are subtracted to suppress the stationary clutter. Figure 5 illustrates the processing steps and data flow of the DPCA technique.

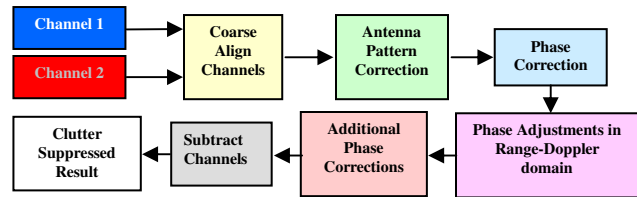


Figure 5. Two-Channel DPCA Processing Flow.

The DPCA algorithm is provided motion compensated phase history data for both the lead (Channel 1) and trailing (Channel 2) channels. Channel 2, the trailing channel data, contains extra pulses to address minor offset delays between the channels. *Alignment* of the range and pulse offset is conducted to roughly get channel 2 to approximate channel 1. Then the antenna patterns are estimated for each channel and an antenna pattern correction is applied to channel 2 so that the channels are similar. A *phase correction* is determined in the Doppler compressed domain to account for differences in the frequency direction not already corrected by coarse channel alignment and to address small phase variations between the channels caused by any minor hardware differences in the collection system. The phase correction factor is applied to the data of channel 2. Further phase adjustments are determined in the range-Doppler domain and applied to channel 2 to account for any shift in the fast-time samples. A series of additional phase corrections are applied to channel 2 by the DPCA algorithm to

improve the fine alignment of channel 2 to channel 1 in an effort to maximize the target-to-clutter ratio. These additional corrections require that any target like objects in the data be avoided so that the target energy is not included in phase correction estimates as was done in the determination of the previous correction factors. This results in a correction for time varying phase differences between both channels being applied to channel 2. Next, a fast-time magnitude and phase correction is applied in the Doppler compressed domain to the data of channel 2. Then a *smoothing technique* is applied to the data resulting in a trailing channel that has been equalized to the lead channel. This completes the alignment process of channel 2 to channel 1. Now that channel 2 appears to be the same as channel 1 the subtraction of the channels result in the cancellation of stationary clutter in the scene. The baseline clutter suppressed data is represented by Eq. 1 below.

$$f_d(k, n) = f_1(k, n) - f_2(k, n) \quad (1)$$

where  $f_1$  is channel 1,  $f_2$  is the equalized phase history data of channel 2 to that of channel 1,  $k$  is the fast-time index,  $n$  is the pulse number, and  $f_d$  is the clutter cancelled result.

The DPCA adaptive clutter cancellation method presented will be applied to the data used in this work to ultimately produce the DPCA 1-D HRR profiles. In an effort to improve the 1-D HRR profiles and preserve more target features, a multi-channel signal subspace technique is developed in Subsection 2.3.

## 2.3 Multi-channel Signal Subspace Technique

The exploitation of the additional information of a third channel in the phased array radar yields more precise clutter estimation and results in better suppression of unwanted clutter returns. By using the information of all three channels, more of the target features are preserved in the clutter canceled image. [42] Increasing available target features should translate into better target identification performance further down the data processing chain. This section will briefly explain the background, the theory behind two channel clutter suppression, and extend this technique to three channel clutter cancellation.

### 2.3.1 Signal Subspace Background

The multichannel signal subspace (MSS) technique is based on 2-D adaptive filtering principles. The process has been applied to a wide variety of data processing problems in the literature [43] such as SAR change detection, [44] image fusion of radar surveillance data, [45,46] medical imaging, and video processing. [47, 48] Most of the work with signal subspace processing has focused on data pairs either separated spatially (e.g. two channel phased array radar data) or separated temporally (e.g. such as electro-optical images collected at different times) as discussed in the literature by Soumekh and others. [43, 46, 49]

The development of a true multi-channel, greater than 2, signal subspace algorithm for use with a multi-channel radar system consisting of a planar antenna array of 22 receiver channels seemed likely.[50] However, the received power at each channel was too weak to form an image of sufficient quality for further processing. This issue was resolved by splitting the data from the 22 channels into a pair of 11 receiver channel groups that were summed to improve the signal to noise level.[46] Once the planar antenna array is represented by two receive channels, the signal subspace processing technique is applied to clutter cancel the data. In the next section, the process for two channel clutter suppression will be explained.

### 2.3.2 Dual Channel Signal Subspace Technique

The dual channel radar system discussed in this section will have a pair of antennas in a phased array similar to what is illustrated in Figure 3, but without the third channel being present. Channel 1 will be the lead channel and channel 2 will be the trailing channel. In keeping with the convention found in the literature, let  $f_1(x, y)$  represent the range-Doppler image formed from the motion-compensated data from channel 1 over a coherent processing interval (CPI) of 128 ms. Then  $f_2(x, y)$  will be the range-Doppler image formed from the motion-compensated data from channel 2 after a slow-time alignment with channel 1. Since the channel 2 range-Doppler image is a linear combination of channel 1 and any shifted versions,  $f_2(x, y)$ , can then be modeled by Eq. 2.[43, 47, 48]

$$f_2(x, y) = f_1(x, y) \otimes h(x, y) + f_e(x, y) \quad (2)$$

where  $f_e(x, y)$  represents the target motion in the range-Doppler image and  $h(x, y)$  is the impulse response representing the relative shift in each range-Doppler image due to differences in the two receive channels of the sensor system.

Gain and phase ambiguities caused by known and unknown factors, such as differences between the antenna patterns or antenna vibration, in the two receive channels may dominate the moving target signature in the imagery. These differences are treated as an error signal in the collected data. The DPCA approach reduces the error signal to a set of pre-determined functions that are estimated and accounted for deterministically. The MSS technique applied to a dual antenna sensor system views the error estimation process as completely stochastic.

Signal subspace theory estimates  $h(x, y)$  from  $f_1(x, y)$  and  $f_2(x, y)$  resulting in the error function,  $\hat{h}(x, y)$ . [43, 45, 47] This is accomplished by minimizing the squared error between  $f_2(x, y)$  and its estimated version given by

$$\hat{f}_2(x, y) = \hat{h}(x, y) \otimes f_1(x, y) \quad (3)$$

where  $\hat{f}_2(x, y)$  is determined by projecting  $f_2(x, y)$  on to a set of orthogonal basis functions defined by  $f_1(x, y)$ . [43] The orthogonal basis functions can be computed using any one of accepted decomposition/orthogonalization techniques such as singular value decomposition, QR orthogonalization, and the Gram-Schmidt procedure to name a few. QR orthogonalization was used in the MSS implementation that generated the results of this paper where in practice  $\hat{h}(x, y) \otimes f_1(x, y)$  is estimated instead of  $\hat{h}(x, y)$ . In general, the spatially-invariant difference over the entire image is represented by Eq. 4 below. [43, 48]

$$\hat{f}_d(x, y) = f_2(x, y) - \hat{f}_2(x, y) \quad (4)$$

To suppress unwanted clutter in radar data, the error function is estimated on overlapping odd-sized blocks over the entire image to account for the spatially varying nature of the phase in the imagery. The entire range-Doppler image is divided into rectangular blocks containing an odd number of pixels and processed to estimate the error function. The blocks of image pixels were moved so that some portion of the rectangular patch overlapped a previously processed block until the entire subdivided image had been processed. This results in a clutter cancelled image given by Eq. 5 [45] for a two channel phased array radar system.

$$\hat{f}_d(x_i, y_i) = \sum_{l=1}^L [f_2(x_i, y_i) - \hat{f}_2(x_i, y_i)] I_l(x_i, y_i) \quad (5)$$

$L$  is the number of overlapping blocks processed,  $i$  is the odd number of pixels per block, and  $I_l$  is an identity matrix. The MSS implementation in this paper used square patches in the processing represented by  $(x_i, y_i)$ , but in general a rectangular block represented by  $(x_i, y_i)$  could be used for an  $i$  by  $j$  dimensioned block. The next section discusses the extension of this technique to data collected with a three channel phased array radar.

### 2.3.3 Three Channel Signal Subspace Technique

The two channel signal subspace method explained in Subsection 2.3.2 is extended for use with all three channels of the phased array radar depicted in Figure 3. Once again, the lead channel will be channel 1 and the trailing channels will be 2 and 3. The Multi-channel Signal Subspace (MSS) extension to three channels will first project the range-Doppler image formed from the aligned motion compensated data of channel 2,  $f_2(x, y)$ , on to the basis functions defined by the range-Doppler image formed from the motion compensated data of channel 1,  $f_1(x, y)$ , and determine the spatially varying difference,  $\hat{f}_{d2}(x_i, y_i)$  given by Eq. 5. The resulting range-Doppler difference image of channels 1 and 2 is treated as a *new* independent channel,  $f_4(x, y)$ , as shown in equation 6 below.

$$f_4(x, y) = \hat{f}_{d2}(x, y) = f_2(x, y) - \hat{f}_2(x, y) \quad (6)$$

Then the range-Doppler image formed by the aligned motion compensated data of channel 3,  $f_3(x, y)$ , is projected on to the basis functions defined by the range-Doppler image formed from the motion compensated data of channel 2,  $f_2(x, y)$ . The spatially varying difference,  $\hat{f}_{d3}(x_i, y_i)$  from (5) is then determined. The resulting range-Doppler difference image of channels 2 and 3 in equation 7 is treated as a second *new* independent channel,  $f_5(x, y)$ , at a slightly different look angle.

$$f_5(x, y) = \hat{f}_{d3}(x, y) = f_3(x, y) - \hat{f}_3(x, y) \quad (7)$$

Now the second *new* independent channel,  $f_5(x, y)$ , is projected on to the orthogonal basis functions of the first *new* independent channel,  $f_4(x, y)$ , represented by Eq. 8.

$$\hat{f}_5(x, y) = f_4(x, y) \otimes \hat{h}_{45}(x, y) \quad (8)$$

Eq. 9 represents the three channel spatially-invariant difference image. The block processing represented by Eq. 5 was applied to account for the spatially varying nature of the range-Doppler images.

$$\hat{f}_d(x, y) = f_5(x, y) - \hat{f}_5(x, y) \quad (9)$$

Since each of the *new* independent channels is essentially a clutter canceled range-Doppler image, this technique represents the fusion of two dual channel clutter suppressed range-Doppler images. The resulting *clutter suppressed* range-Doppler image should contain more target features from the slightly different viewing antenna geometries in the array. The MSS method improves target features without enhancing any residual clutter in the *new* input images. Examples of this processing are presented in the section that follows.

## 2.4 Clutter Suppression Results

The clutter suppressed range-Doppler chips presented in this section were generated from the same part of the collected data discussed in Subsection 2.1. The moving target, a sedan, is slowing down while heading south, away from the radars' location. All of the range-Doppler chips presented in this section have a dynamic range of 50 dB with Doppler increasing from the left of the image to right and range increasing from the bottom of the image to the top. The DPCA algorithm result is presented first, then the 2 channel MSS processed chips, and finally the 3 channel clutter suppressed result. The signal-to-noise level for all of the clutter suppressed range-Doppler chips is computed for algorithm performance comparison.

The implementation of the DPCA algorithm required the first channel to be the lead channel and limited the amount

of shifting that may occur to align the two channels. Therefore, only channels 1 and 2 could be processed to yield a clutter cancelled range-Doppler image. The result is shown in **Figure 6**. As stated earlier, the dynamic range is constant for all the results present in this section. However, adjusting the dynamic range of the DPCA range-Doppler chip would help better define the target.

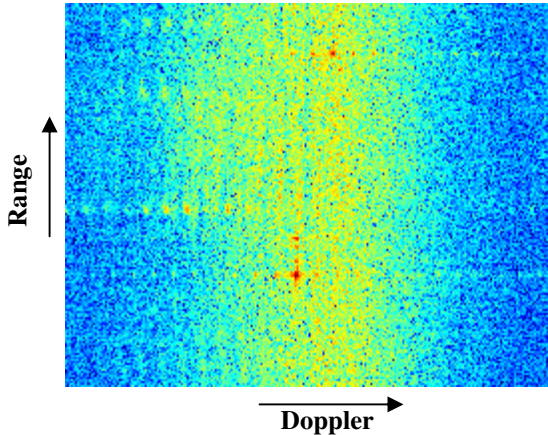


**Figure 6.** DPCA clutter suppression technique.

Although the DPCA method could only produce clutter cancelled chips from two of the three channels available, the multi-channel signal subspace (MSS) technique utilized all three channels in the processing. **Figure 7** is the clutter suppressed range-Doppler image produced from channels 1 and 2. In comparing **Figure 7** to **Figure 6**, the MSS approach does a better job of clutter cancellation than the baseline technique using the same data channels.

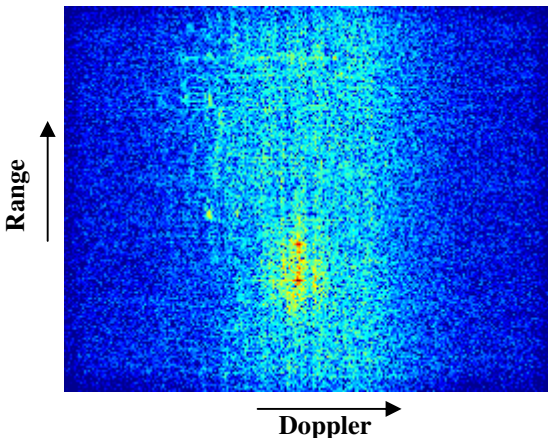


**Figure 7.** MSS Two channel clutter suppression technique: channels 1 & 2.

In **Figure 8** the clutter cancelled result of the MSS algorithm using channels 2 and 3 is presented. The relative reduction of clutter is similar to that of **Figure 7**. Close examination of **Figures 7** and **8** reveal scattering from different locations of the target as well as more features in the range-Doppler imagery. This is caused in part by minor variations in the collection geometry due to the spacing of the antennas in the phased array radar.

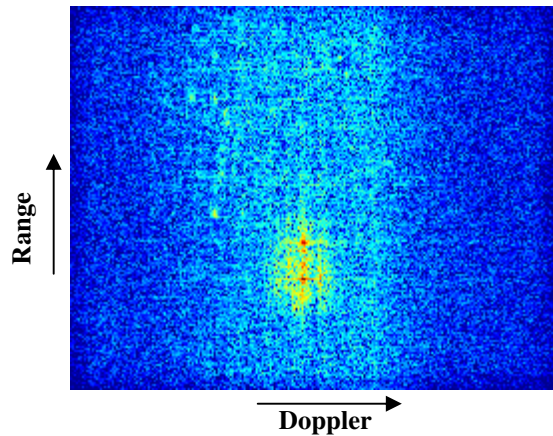


**Figure 8.** MSS Two channel clutter suppression technique: channels 2 & 3.

Found in **Figure 9** is the clutter suppressed range-Doppler chip produced by the enhanced MSS algorithm using all three channels of motion compensated data. A minor reduction in the level of clutter cancellation can be seen when comparing the results of **Figure 9** to that of **Figures 7** and **8**. However, careful examination of the range-Doppler image in **Figure 9** shows more target features are present. The three channel clutter suppressed image has a signal to noise level comparable to that of the MSS 2 channel clutter cancelled results and is an improvement over the baseline technique.

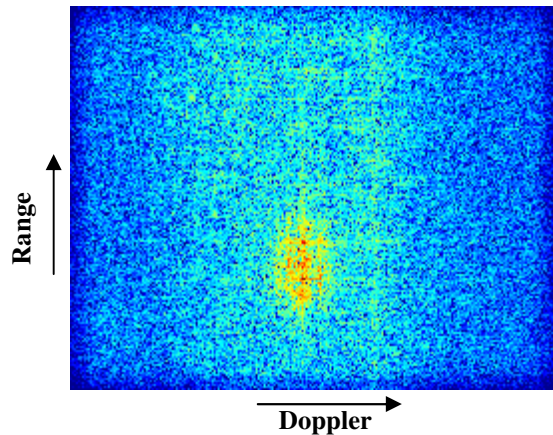


**Figure 9.** MSS Three channel clutter suppression technique.

Finally, a signal-to-clutter ratio was determined for the chips presented in this section to help gauge the relative performance levels of the various techniques. This ratio was determined by finding the largest pixel value in the image which is the brightest point on the target and dividing it by the average clutter in a one pixel wide frame around the entire range-Doppler chip. A comparison of the signal to clutter levels for the range-Doppler images formed from the three techniques discussed in this paper can be found in **Table 1**.

DPCA processing	33.20 dB
MSS: 2 channel signal subspace: ch. 1 & 2	42.81 dB
MSS: 2 channel signal subspace: ch. 2 & 3	42.99 dB
MSS: 3 channel signal subspace	42.57 dB

**Table 1.** DPCA vs. MSS Target to Clutter Ratio Comparison.

The MSS performance scales based on the comparable target to clutter ratios for both the two channel and three channel processing, with the three channel MSS method resulting in a slightly noisier clutter suppressed image, but with the added benefit of more target features being preserved after clutter cancellation. The results of this section indicate that the MSS technique for traditional two channel clutter cancellation and for multi-channel clutter suppression performs much better than the DPCA method.

### 3 Identification Performance

Single-look confusion matrices were produced for 1-D HRR profiles formed from DPCA and MSS clutter canceled target chips for a scenario where ten ground vehicles were traveling along the roads shown in **Figure 4**. Obscuration from nearby vegetation along the streets impacted identification performance depending on collection geometry. The results of these experiments are presented in the subsections that follow.

#### 3.1 DPCA Single-Look Performance

Five vehicles were selected for the library and the remaining five vehicles were used as confusers. The DPCA single-look identification results are shown in **Figure 10** with a mean target recognition rate of 65%. The distribution of the confuser vehicles is spread across the not-in-library row of confusion matrix indicating no strong bias toward a library object.

	DPCA Identification Performance					
	TARGET 1	TARGET 2	TARGET 3	TARGET 4	TARGET 5	OTHER
TARGET 1	0.63	0.075	0.12	0.056	0.042	0.084
TARGET 2	0.039	0.67	0.068	0.11	0.091	0.02
TARGET 3	0.047	0.1	0.7	0.07	0.027	0.054
TARGET 4	0.081	0.077	0.074	0.62	0.11	0.039
TARGET 5	0.12	0.088	0.051	0.088	0.63	0.025
NOT-IN-LIB	0.21	0.099	0.22	0.19	0.063	0.21

**Figure 10.** DPCA Single-Look Performance.

#### 3.2 MSS Single-look Performance

The 3 channel MSS single-look 1-D HRR ATR performance is presented in **Figure 11** with an improved mean recognition rate of 73.6% relative to the DPCA

results. Once again the distribution of the confuser vehicles is spread across the not-in-library row for the MSS confusion matrix indicating no strong bias toward a library object. The off diagonal target confusion is somewhat reduced relative to the DPCA processed data in **Figure 10**.

	MSS Identification Performance					
	TARGET 1	TARGET 2	TARGET 3	TARGET 4	TARGET 5	OTHER
TARGET 1	0.74	0.079	0.048	0.028	0.08	0.025
TARGET 2	0.028	0.79	0.031	0.052	0.076	0.023
TARGET 3	0.02	0.092	0.78	0.021	0.037	0.052
TARGET 4	0.022	0.074	0.089	0.65	0.08	0.082
TARGET 5	0.077	0.047	0.032	0.04	0.72	0.087
NOT-IN-LIB	0.25	0.18	0.15	0.071	0.11	0.24

**Figure 11.** 3 Channel MSS Single-Look Performance.

## 4 Discussion & Conclusions

The capability to collect and process three channels of radar data from a system configured with three phased array antennas oriented in the along-track dimension has been demonstrated. The application of traditionally accepted two channel clutter suppression techniques has been extended to true multi-channel data. The Multichannel Signal Subspace (MSS) technique for two channels of data was demonstrated to be a superior clutter suppression technique to that of the DPCA method. The MSS methodology was extended to exploit the additional information provided by the third channel of the phased array interrogating the scene.

The MSS technique applied to three channels of data suppressed the clutter very well while preserving the features of the moving target. The signal-to-noise level of the three channel MSS technique is approximately that of the two channel MSS results. The availability of more target features in the range-Doppler image while maintaining a good clutter suppression level makes the MSS approach beneficial to ATR applications. A significant ATR performance improvement is achieved with clutter suppressed data using the MSS algorithm relative to ATR performance with DPCA suppressed data.

A major factor not addressed in this paper, however; is that the processing time for the MSS algorithm is quite significant, especially when compared to the DPCA method. The processing times will need to be drastically reduced for the MSS algorithm to be practical in a data processing or operation environment. A potential solution is the parallelization of the time consuming block processing steps. This remains an area of future study.

Next steps include multi-look decision-level and feature-level fusion using the MSS technique for simultaneous tracking and identification.

## 5 References

- [1] E. Blasch, *Derivation of A Belief Filter for High Range Resolution Radar Simultaneous Target Tracking and Identification*, Ph.D. Diss., Wright State University, 1999.
- [2] E. Blasch and C. Yang, "Ten methods to Fuse GMTI and HRRR Measurements for Joint Tracking and ID", *Fusion 04*, July 2004.
- [3] Y. Bar-Shalom & X. Li, *Multitarget-Multisensor Tracking: Principles and Techniques*, YBS, New York, 1995.
- [4] S. Blackman and R. Popoli, *Design and Analysis of Modern Tracking Systems*, Artech House Publisher, Boston, 1999.
- [5] S. G. Nikolov, E. Fernandez Canga, J. J. Lewis, A. Loza, D. R. Bull, and C. N. Canagarajah, "Adaptive Image Fusion Using Wavelets: Algorithms and System Design", in *Multisensor Data and Information Processing for Rapid and Robust Situation and Threat Assessment*, Eds. E. Lefebvre, P. Valin, IOS Press, 2006.
- [6] D. Gross, M. Oppenheimer, B. Kahler, B. Keaffaber, and R. Williams, "Preliminary Comparison of HRR Signatures of Moving and Stationary Ground Vehicles", *Proc. SPIE*, Vol. 4727, 2002.
- [7] H-C. Chiang, R.L. Moses, and L.C Potter, "Model based classification of radar images", *IEEE Transactions on Information Theory*, 46, 5 (2000), 1842-1854.
- [8] B. Kahler and E. Blasch, "Robust Multi-Look HRR ATR Investigation Through Decision-Level Fusion Evaluation", *Proc. 11<sup>th</sup> International Conference On Information Fusion*, July 2008.
- [9] B. Kahler, J. Querns, G. Arnold, "An ATR Challenge Problem Using HRR Data", *Proc. SPIE*, Vol. 6970, 2008.
- [10] R. Williams, J. Westerkamp, D. Gross, and A. Palomino, "Automatic Target Recognition of Time Critical Moving Targets Using 1D High Range Resolution (HRR) Radar", *IEEE AES Systems Magazine*, April 2000.
- [11] R. Wu, Q. Gao, J. Liu, and H. Gu, "ATR Scheme Based On 1-D HRR Profiles", *Electronic Letters*, Vol. 38, Issue 24, Nov. 2002.
- [12] S. Paul, A. K. Shaw, K. Das, and A. K. Mitra, "Improved HRR-ATR Using Hybridization Of HMM and Eigen-Template-Matched Filtering", *IEEE Conf. on Aco., Speech, and Sig. Proc.*, 2003.
- [13] R.A. Mitchell and J.J. Westerkamp, "Robust Statistical feature based aircraft identification", *IEEE Trans. on Aerospace & Electronic Systems*, 35, 3, 1999.
- [14] E. Blasch, J.J. Westerkamp, J.R. Layne, L. Hong, F. D. Garber and A. Shaw, "Identifying moving HRR signatures with an ATR Belief Filter," *SPIE* 2000.
- [15] E. Blasch and M. Bryant, "SAR Information Exploitation Using an Information Filter Metric," *IEEE*, 1998.
- [16] E. Blasch and S. Huang, "Multilevel Feature-based fuzzy fusion for target recognition," *Proc. SPIE* 2000.
- [17] E. Blasch, and L. Hong, "Data Association through Fusion of Target Track and Identification Sets," *Fusion00*.
- [18] W. Snyder, G. Ettinger and S. Laprise, "Modeling Performance and Image Collection Utility for Multiple Look ATR", *Proc SPIE* 2003.
- [19] K. Shaw and V. Bhatnagar, "Automatic Target Recognition using Eigen-Templates", *Proc. of SPIE*, Vol. 3370, 1998.
- [20] B. V. K. Vijaya Kumar and M. Alkanhal, "Eigen-extended Maximum Average Correlation Height (EEMACH) Filters For Automatic Target Recognition", *Proc. SPIE*, Vol. 4379, 2001.
- [21] F. Dicander and R. Jonsson, "Comparison of Some HRR-Classification Algorithms", *Proc. SPIE*, Vol. 4382, 2001.
- [22] B. Kahler, E. Blasch, L. Goodwon, "Operating Condition Modeling for ATR Fusion Assessment", *Multisensor, Multisource Information Fusion*, Vol. 6571, April 2007.
- [23] J. Lancaster, S. Blackman, "Joint IMM/MHT Tracking and Identification for MultiSensor Ground Tracking, Fusion06, 2006.
- [24] S. Mori, C-Y. Chong, E. Tse, and E. P. Wishner, "Tracking and Classifying Multiple Targets Without A Priori Identification," *IEEE Trans. On Automatic Control*, Vol. AC-31, No. 5, May 1986.
- [25] D. Angelova & L. Mihaylova, "Joint Tracking and Classification with Particle Filtering and Mixture Kalman Filtering using Kinematic Radar Information," *Digital Signal Processing*, 2005.
- [26] A. Tchamova, J. Dezert, et al, "Target Tracking with Generalized data association based on the general DS<sub>m</sub> rule of combination," *Fusion04*, 2004.
- [27] L. E. Brennan and L. S. Reed, "Theory Of Adaptive Radar", *IEEE Transactions On Aerospace And Electronic Systems*, Vol. AES-9, No. 2, March 1973, pp. 237 – 252.
- [28] B. Liu, "Clutter Suppression Using Recursive and Nonrecursive MTI Filters", *IEEE Transactions on Aerospace and Electronic Systems*, Vol. 24, No. 3, May 1988, pp. 210 – 217.
- [29] J. K. Jao, "Theory of Synthetic Aperture Radar Imaging of a Moving Target", *IEEE Transactions on Geoscience and Remote Sensing*, vol. 39, No. 9, Sept. 2001, pp. 1984 - 1992.
- [30] R. Klemm, "Introduction to space-time adaptive processing", *IEE Electronics & Communication Engineering Journal*, Feb. 1999.
- [31] R. Klemm, "Prospectives In STAP Research", *Proc. Of the 2000 IEEE Sensor Array and Multichannel Signal Processing Workshop*, March 2000, pp. 7-11.
- [32] P. G. Richardson, "Effects of Manoeuvre on Space Time Adaptive Processing Performance", *IEEE Radar 97 Conf.*, Pub. No. 449, Oct. 1997, pp. 285-289.
- [33] T. Nohara, "Comparison of DPCA and STAP for Space-Based Radar", *IEEE International Radar Conference*, 1995, pp. 113-119.
- [34] P. G. Richardson, "Analysis of the Adaptive Space Time Processing Technique for Airborne Radar", *IEE Proc. - Radar, Sonar Navig.*, Vol. 141, No. 4, Aug. 1994, pp. 187 – 195.
- [35] D. J. Choe and R.G. White, "Moving Target Detection in SAR Imagery: Experimental Results", *IEEE International Radar Conference*, 1995, pp. 644 – 649.
- [36] C.E. Muehe and M. Labitt, "Displaced-Phase-Center Antenna Technique", *Lincoln Laboratory Journal*, Vol. 12, No. 2, 2000.
- [37] G. Krieger, N. Gebert, and A. Moreira, "Unambiguous SAR Signal Reconstruction From Nonuniform Displaced Phase Center Sampling", *IEEE Geoscience and Remote Sensing Letters*, Vol. 1, No. 4, Oct. 2004, pp.260-264.
- [38] T. Nohara, P. Scarlett, and B. Eatock, "A Radar Signal Processor for Space-Based Radar", *IEEE 1993 National Radar Conference*.
- [39] W. E. Ng, C. B. Zhang, Y. H. Lu, T. S. Yeo, "Simulated DPCA Performance for Dual-Channel SAR Processing", *IEEE*, 1999.
- [40] M. Soumekh, S. Worrell, E. Zelnio, and B. Keaffaber, "SAR Wavefront Reconstruction Using Motion Compensated Phase History (Polar Format) Data and DPCA-Based GMTI", *Algorithms for Synthetic Aperture Radar Imagery VII, Proc. Of SPIE*, Vol. 4053, April 2000, pp. 64 - 75.
- [41] T. Nohara, "Derivation of a 3-Channel DCPA/Monopulse Radar using Phased Arrays", *IEEE National Telesystems Conference*, 1994, pp. 243 – 246.
- [42] B. Kahler, B. Keaffaber, "An Improved Multi-Channel Clutter Suppression Algorithm", *Algorithms for Synthetic Aperture Radar Imagery XIV, Proc. Of SPIE*, Vol. 6568, April 2007.
- [43] M. Soumekh, "Signal Subspace Fusion of Uncalibrated Sensors with Application in SAR, Diagnostic Medicine and Video Processing, in *Proc. ICIP*, Santa Barbara, CA, Oct. 1997.
- [44] K. Ranney and M. Soumekh, "Signal Subspace Change Detection in Averaged Multi-Look SAR Imagery", *Algorithms for Synthetic Aperture Radar Imagery XII, Proc. Of SPIE*, 2005, pp. 222-233.
- [45] M. Soumekh, "Moving Target Detection and Imaging Using an X Band Along-Track Monopulse SAR", *IEEE Transactions on Aerospace and Electronic Systems*, Vol. 38, No. 1, Jan. 2002.
- [46] M. Soumekh and B. Himed, "SAR-MTI Processing of Multi-Channel Airborne Radar Measurement (MCARM) Data", *Proc. IEEE Radar Conference*, Long Beach, May 2002.
- [47] M. Soumekh, "Signal Subspace Fusion of Uncalibrated Sensors with Application in SAR and Diagnostic Medicine", *IEEE Transaction on Image Processing*, Vol. 8, No. 1, Jan. 1999.
- [48] X. Guo and M. Soumekh, "Signal Subspace Registration of Time Series Medical Imagery", in *Proc. ICSP*, 2002, pp. 1524-1527.
- [49] M. Soumekh, *Synthetic Aperture Radar with MATLAB Algorithms*. New York, NY 10158-0012:John Wiley & Sons, Inc., 1999.
- [50] B. N. S. Babu, J. A. Torres, and W. L. Melvin, "Processing and evaluation of multichannel airborne radar measurements (MCARM) measured data", *IEEE International Symposium on Phased Array Systems and Technology*, 15-18 Oct. 1996.